Journal of Cellular Biochemistry 100:385–401 (2007)

PARP-3 Associates With Polycomb Group Bodies and With Components of the DNA Damage Repair Machinery

M. Rouleau,[1] D. McDonald,[2] P. Gagné,[1] M.-E. Ouellet,[1] A. Droit,[1] J.M. Hunter,[1] S. Dutertre,[3] C. Prigent,[4] M.J. Hendzel,[2] and G.G. Poirier[1]*

[1]Health and Environment Unit, Laval University Medical Research Centre, CHUQ, Faculty of Medicine, Laval University, 2705 Blvd Laurier, Sainte-Foy, Québec, G1V 4G2, Canada
[2]Department of Oncology, Faculty of Medicine, University of Alberta and Cross Cancer Institute, Alberta, T6G 1Z2, Canada
[3]IFR140, Microscopy plateform, Université de Rennes I, 2 avenue du Pr Léon Bernard, 35043 Rennes, France
[4]CNRS UMR6061, Groupe Cycle Cellulaire, IFR140, Université de Rennes I, 2 avenue du Pr Léon Bernard, 35043 Rennes, France

Abstract Poly(ADP-ribose) polymerase 3 (PARP-3) is a novel member of the PARP family of enzymes that synthesize poly(ADP-ribose) on themselves and other acceptor proteins. Very little is known about this PARP, which is closely related to PARP-1 and PARP-2. By sequence analysis, we find that PARP-3 may be expressed in two isoforms which we studied in more detail to gain insight into their possible functions. We find that both PARP-3 isoforms, transiently expressed as GFP or FLAG fusions, are nuclear. Detection of endogenous PARP-3 with a specific antibody also shows a widespread nuclear distribution, appearing in numerous small foci and a small number of larger foci. Through co-localization experiments and immunoprecipitations, the larger nuclear foci were identified as Polycomb group bodies (PcG bodies) and we found that PARP-3 is part of Polycomb group protein complexes. Furthermore, using a proteomics approach, we determined that both PARP-3 isoforms are part of complexes comprising DNA-PKcs, PARP-1, DNA ligase III, DNA ligase IV, Ku70, and Ku80. Our findings suggest that PARP-3 is a nuclear protein involved in transcriptional silencing and in the cellular response to DNA damage. J. Cell. Biochem. 100: 385–401, 2007.

Key words: PARP; poly(ADP-ribose); Polycomb group; DNA repair; Ku70/Ku80; immunoprecipitation; proteomics; splice variants

Poly(ADP-ribosyl)ation is a post-synthetic protein modification where long chains of ADP-ribose are synthesized by poly(ADP-ribose) polymerases (PARPs) at the expense of NAD+. Poly(ADP-ribose) is short lived owing to the activity of a poly(ADP-ribose) glycohydrolase (PARG), which catabolizes the polymer within minutes after synthesis [Alvarez-Gonzalez and Althaus, 1989]. The PARP family may be comprised of as many as 16 members which share a common catalytic domain responsible for the synthesis of poly(ADP-ribose) [Amé et al., 2004; Otto et al., 2005]. The best characterized and abundant member is PARP-1, a 113 kDa nuclear protein comprising a DNA-binding domain specified by two zinc fingers that allow PARP-1 to be rapidly activated in response to DNA damage. A number of nuclear proteins have been identified as substrates of PARP-1, with histones and PARP-1 being the preferred

This article contains supplementary material, which may be viewed at the Journal of Cellular Biochemistry website at http://www.interscience.wiley.com/jpages/0730-2312/suppmat/index.html.

Grant sponsor: Canadian Institutes for Health Research; Grant number: MOP-14052; Grant sponsor: Canadian Chair in Proteomics; Grant sponsor: Canadian Institutes for Health Research; Grant number: MOP-74648.

J.M. Hunter's present address is Caprion Pharmaceuticals, Inc., 7150 Alexander-Fleming, Montreal, Quebec, H4S 2C8, Canada.

*Correspondence to: G.G. Poirier, Health and Environment Unit, Laval University Medical Research Centre, CHUQ, Faculty of Medicine, Laval University, 2705 Blvd Laurier, Sainte-Foy, Québec, G1V 4G2, Canada.
E-mail: guy.poirier@crchul.ulaval.ca

Received 1 May 2006; Accepted 9 June 2006
DOI 10.1002/jcb.21051

substrates [Ogata et al., 1981; Boulikas, 1990; reviewed by D'Amours et al., 1999]. Despite the transient accumulation of poly(ADP-ribose), it has an important function in chromatin remodeling, DNA damage repair, regulation of transcription and cell division [Tulin and Spradling, 2003; Chang et al., 2004; Dynek and Smith, 2004; Ju et al., 2004; Kim et al., 2004; reviewed by Rouleau et al., 2004].

Few other members of the PARP family have been studied. PARP-2 is a 62 kDa nuclear PARP comprising a small DNA-binding domain. It is activated by DNA damage, capable of automodification and interacts with several members of the base excision DNA repair machinery including PARP-1 [Amé et al., 1999; Schreiber et al., 2002]. PARP-2 has partially redundant functions with PARP-1 [Schreiber et al., 2002; Ménissier-de Murcia et al., 2003; Meder et al., 2005]. This functional overlap is essential for the survival of PARP-1 null mice because PARP-1/PARP-2 null mice are not viable [Shall and de Murcia, 2000; Ménissier-de Murcia et al., 2003; Huber et al., 2004]. In addition, recent evidence has been gathered that PARP-2 is involved in the maintenance of telomeric integrity through a functional interaction with the telomeric protein TRF2 [Dantzer et al., 2004] and in the regulation of the transcriptional activity of thyroid transcription factor-1 [Maeda et al., 2006]. Vault PARP (VPARP, 193 kDa) is a constituent of vault particles, which are cytoplasmic ribonucleoprotein complexes that may have a transport function [Kickhoefer et al., 1999]. Some VPARP also localizes to the mitotic spindle in mitotic cells [Kickhoefer et al., 1999]. The function of VPARP remains undefined. Tankyrases constitute a subfamily of PARP enzymes [Amé et al., 2004]. Tankyrase 1 (142 kDa) and tankyrase 2 (127 kDa) are found at telomeres where they poly(ADP-ribosyl)ate the negative regulator of telomere length TRF-1, causing its release from telomeres and facilitating telomere elongation. They also interact with insulin responsive amino peptidase in the Golgi and contribute to the regulation of vesicle trafficking [Smith and de Lange, 1999; Chi and Lodish, 2000; Cook et al., 2002; Sbodio et al., 2002]. Tankyrase 1 has also been found associated with nuclear pores and centrosomes [Smith and de Lange, 1999]. Recently, the PARP activity of tankyrase 1 was shown essential for the resolution of sister telomeres during mitosis. Tankyrase 1 is believed to disrupt a "telomere cohesion complex" that holds telomeres together until separation at anaphase [Dynek and Smith, 2004]. This observation highlighted a novel important function of poly(ADP-ribosyl)ation. Finally, PARP-10, which is a new addition to the PARP family, is a partner of the proto-oncoprotein *c*-Myc, a protein that regulates cellular proliferation [Yu et al., 2005].

The sequence of PARP-3 is most related to that of PARP-1 and PARP-2. First identified as a putative 533 amino acid PARP [Johansson, 1999], an analysis of the genomic organization of the human ADPRTL3 gene revealed that a second, seven amino acid longer, PARP-3 isoform could be expressed owing to alternative splicing [Urbanek et al., 2002]. A recent characterization of the longer PARP-3 isoform revealed that it is a DNA-independent PARP that specifically resides in centrosomes [Augustin et al., 2003]. In this report, we extend the knowledge on human PARP-3 by showing that both PARP-3 isoforms are preferentially nuclear with no discernable association with the centrosome. We also find that PARP-3 is part of Polycomb group bodies and of protein complexes that comprise proteins of non-homologous end-joining and base excision DNA repair pathways.

MATERIALS AND METHODS

Cell Culture

COS-7 and HeLa cells were grown at 37°C in a 5% CO_2 environment in DMEM (Invitrogen Corp.) supplemented with 1% Glutamax (Invitrogen), 10% fetal bovine serum (FBS, Wisent), 100 IU/ml penicillin, and 100 μg/ml streptomycin (Invitrogen).

PARP-3 Constructs

A GeneStorm® clone (accession number M15131) comprising the coding sequence of the short isoform of human PARP-3 (hPARP-3_{short}) was obtained from ResGen (Invitrogen). To allow the transient expression of hPARP-3 isoforms in fusion with the FLAG epitope or the green fluorescent protein (GFP) at their N-terminus in mammalian cells, the following constructs were made. The pFLAG-hPARP-3_{short} plasmid was constructed by PCR cloning using the following upper primer 1: 5′-CGGAATTC-TATGGCTCCAAAGCCGAAGCCCTGG and lower primer 2: 5′-CGCGAAGCTTTTACTA-GAGGTGGACCTCCAGCAGGTAGCG using

the PARP-3 GenStorm® clone as a template. The PCR product was digested with *Eco*RI and *Hind*III and subcloned in pCMV-Tag2A (Stratagene) cut with the same enzymes. The pFLAG-hPARP-3_{long} plasmid was constructed with an identical strategy using upper primer 3 (5′-CGGAATTCTATGTCCCTGCTTTTCTTGGCCATGGCTCCAAAGCCGAAGCCC) in combination with lower primer 2 for PCR amplification. PCR using upper primer 1 and lower primer no. 4 (5′-CGGGTACCTTACTAGAGGTGGACCTCCAGCAGGTAGCG) for amplification of hPARP-3_{short} and using upper primer 3 and lower primer 4 for amplification of hPARP-3_{long} allowed to generate pGFP-hPARP-3_{short} and pGFP-hPARP-3_{long} plasmids by digestion of amplified PCR products with *Eco*RI and *Kpn*I and ligation in the vector pEGFP-C1 (Clontech) cut with the same enzymes. The sequence of each construction was verified by automated sequencing performed at the sequencing facility of the Research Center.

pFLAG-hPARP-3_{short} was cut with *Not*I and *Xho*I and this fragment was ligated into the pShuttle-IRES-hrGFP-1 vector of the AdEasy XL adenoviral vector system to generate a recombinant adenovirus as described by the manufacturer (Stratagene). Recombinant adenoviruses were generated at the Viral Vector Core Facility (University of Ottawa). To infect cells with the recombinant adenovirus driving the expression of FLAG-hPARP-3_{short} (AdFP3), HeLa or COS-7 cells were grown in 15 cm Petridish to 50% confluence. Cells were rinsed with PBS and 8 ml DMEM supplemented with Glutamax containing 10 viral particles/cell (multiplicity of infection, MOI) were added to the culture dish. Cells were incubated for 4 h with occasional shaking after which 17 DMEM supplemented with Glutamax and 5% FBS were added to the culture dish. Cells were harvested 24 h post-infection as described below. Infections with AdGFP, a control recombinant adenovirus expressing GFP, was carried out in similar conditions.

Ku70 Construct

The coding sequence of Ku70 was amplified by PCR using upper primer 5 (5′-CGGGATCCATGTCAGGGTGGGAGTCATA) and lower primer 6 (5′-GGCTCGAGTCAGTCCTGGAAGTGCTTGG) and the I.M.A.G.E. clone 3448510 comprising the full length Ku70 sequence (obtained from the American Type Culture Collection) as a template. The PCR product was digested with *Bam*HI and *Xho*I and subcloned in pCMV-Tag3B (Stratagene) cut with the same enzymes to generate pMyc-Ku70. The sequence of pMyc-Ku70 was verified as above.

Generation of Anti-PARP-3 Antibodies

The peptide K^{24}KGRQAGREEDPFRS^{38} (Fig. 1B) was synthesized with MAP resin 4-branch (ABI) at the peptide synthesis facility of our Research Center. A polyclonal antiserum against PARP-3 was produced by immunization of a New Zealand white rabbit (Charles River) using a standard immunization protocol approved by the animal protection committee of the Centre Hospitalier Universitaire de Québec. At all times, animals were treated according to the guidelines and policies of the Canadian Council on Animal Care (http://www.ccac.ca/en/CCAC_Programs/Guidelines_Policies/gublurb.htm; Olfert et al., 1993). The generated antiserum recognizes by immunofluorescence short and long isoforms of hPARP-3.

Immunofluorescence

COS-7 and HeLa cells grown on coverslips were transfected by a standard calcium phosphate method with pFLAG-hPARP-3_{short}, pFLAG-hPARP-3_{long}, pGFP-hPARP-3_{short} or pGFP-hPARP-3_{long}, or infected with AdFP3 and fixed 24 h after transfection or infection in 4% formaldehyde diluted in PBS for 15 min. Cells expressing FLAG-tagged proteins were washed in PBS and incubated either with M2 (Stratagene) anti-FLAG monoclonal antibody (1:1,000) or anti-PARP-3 antibodies (1:300) for 90 min at room temperature or overnight at 4°C. Cells washed in PBS were then incubated with appropriate FITC- or Texas Red-conjugated anti-mouse or anti-rabbit antibodies (Jackson ImmunoResearch) (1:1,000). Antibodies were diluted in 10% FBS, 1% Triton X-100 in PBS. Cells were washed, counterstained with Hoechst 33342 and mounted with Fluoromount-G (Southern Biotechnology Associates). Cells were viewed with Nikon E1000 or E80i microscopes equipped with a CoolSNAP$_{fx}$ camera (Roper Scientific). Fixed cells expressing GFP-tagged proteins were stained with Hoechst and cells were mounted as described. Images were processed using Metamorph software (Universal Imaging Corp.)

Co-localization of PARP-3 with Polycomb group proteins were conducted by co-staining with anti-PARP-3 and an antibody specific for trimethylated K27 histone H3 (Abcam ab6002; 1:300) or anti-RbAp46/48 (Abcam ab490; 1:400). For co-localization with YY1, HeLa cells were infected with 10 MOI AdFP3, then M2 (1:1,000) and anti-YY1 (Santa Cruz C-20; 1:300) were used to detect FLAG-PARP-3 and YY1 respectively. To assess PARP-3 association with centrosomes, COS-7 cells were transfected with a GFP-centrin construct (GFP-BBS6, a kind gift from Dr. J. Rattner, University of Calgary) using Effectene transfection reagent (Qiagen) prior to staining for endogenous PARP-3 as described above. Alternatively, cells were co-stained with anti-PARP-3 and mouse polyclonal anti-pericentrin or anti-ninein antibodies (kindly provided by Dr. G. Chan, University of Alberta). Cells were viewed with Zeiss AxioplanII motorized microscope equipped with a CoolSnapHQ cooled CCD camera (Photometrics). Images were processed using Metamorph software.

Immunoprecipitations and Protein Identifications

COS-7 and HeLa cells were transfected by a standard calcium phosphate method with pFLAG-hPARP-3_{short} or pFLAG-hPARP-3_{long} or infected with AdFP3 (10 MOI). Control cells consisted of mock-transfected cells or cells infected with AdGFP (10 MOI). Each immunoprecipitation was conducted with 15×10^6 cells, 48 h post-transfection or 24 h post-infection. All steps were carried out at 4°C. Cells were washed with PBS then scrapped from the culture dish in 800 μl lysis buffer (20 mM Tris-HCl, pH 7.4 (4°C), 137 mM NaCl, 1% Triton X-100, 1 mM DTT, protease inhibitors (Complete, Roche)). Cells were collected in Eppendorf tubes and lysed for 1 h on a rotating unit. Lysed cells were spun in a microcentrifuge at 13,000 rpm for 10 min to clear the lysate. M2 (4 μl) and Protein G-conjugated magnetic beads (120 μl; Dynabeads®, Invitrogen) blocked with 1% BSA were added to the cellular extract and incubated for 2 h. Beads were washed four times with lysis buffer. For Western analysis, proteins were eluted by boiling beads in Laemmli sample buffer. For mass spectrometry, beads were washed once with TBS (10 mM Tris-HCl, pH 7.4, 150 mM NaCl) prior to elution of immunoprecipitated proteins in 140 μl TBS containing 120 μg FLAG synthetic peptide for 6 h. Eluted proteins were boiled in Laemmli sample buffer and separated on an 8% polyacrylamide gel.

Immunoprecipitation of myc-Ku70 was carried out as described for FLAG-hPARP-3 using the anti-Myc tag antibody (clone 4A6, Upstate). COS-7 cells were co-transfected with pMyc-Ku70 and pFLAG-hPARP-3_{short} using the calcium phosphate method. Expression was allowed to occur for 48 h prior to lysis of cells and immunoprecipitation. Detection of immunoprecipitated proteins was by Western blotting.

To assess the dependence of protein-FLAG-hPARP-3 interactions on nucleic acids, cell lysates were treated with Benzonase® (Novagen), a highly purified endonuclease that degrades all forms of DNA and RNA. $MgCl_2$ (final concentration 1 mM) and 25 U Benzonase® were added to a cleared lysate from 1×10^6 COS-7 cells. The treated lysate was then incubated for 20 min at 30°C prior to the immunoprecipitation of FLAG-hPARP-3_{short} with M2 as described above.

Detection and identification of immunoprecipitated proteins was carried out by Western blotting and mass spectrometry. For Western blotting, proteins were transferred to PVDF membranes and incubated with M2 (1:5,000), anti-Ku80 (1:5,000; clone 111, Oncogene Research), anti-Ku70 (1:3,000; a kind gift from Dr. S. Lees-Miller, University of Calgary), anti-PARP-1 (1:5,000; clone C_{II}-10), anti-DNA-PKcs (1:5,000; clone 18-2, Oncogene Research), anti-YY1 (1:2,500; C-20, Santa Cruz), anti-Suz12 (1:2,500; Upstate), anti-EZH2 (1:2,500, clone 11, BD Pharmingen), anti-hdac1 (1:3,000, Abcam), anti-hdac2 (1:2,000, Santa Cruz) then with the appropriate secondary antibody conjugated to peroxidase and revealed by chemiluminescence detection (Perkin Elmer). For LC-MS/MS (liquid chromatography–tandem MS) analysis, gels were stained with Sypro Ruby protein stain (Bio-Rad) according to manufacturer's instructions and scanned with a PROXpress (Perkin Elmer), a CCD-based imaging system. Protein bands were cut manually under UV illumination. In-gel protein digests were performed on a MassPrep liquid handling station (Micromass) according to the manufacturer's protocol and using sequencing-grade modified trypsin (Promega). Peptide extracts were dried out using a SpeedVac and resuspended in 10 μl of 0.1% formic acid in water.

Final extracts were analysed by LC-MS/MS using an LCQ-DECA XP mass spectrometer equipped with a nanospray source and a Surveyor HPLC system (Thermo Electron). MS/MS spectra were searched using the SEQUEST [Eng et al., 1994] search engine and the algorithms PeptideProphet [Keller et al., 2002] and ProteinProphet [Nesvizhskii et al., 2003] were subsequently used to determine the probability that peptide and protein assignments were correct. PeptideProphet provides an empirical statistical model which estimates the accuracy of peptide identifications made by SEQUEST. ProteinProphet subsequently groups the assigned peptides according to corresponding proteins and computes a probability of a correct protein assignment for each protein [Nesvizhskii et al., 2003; von Haller et al., 2003]. In order to maximize protein coverage, a two-pass strategy was used. For the first pass, MS/MS spectra were searched against protein sequences of the International Protein Index human dataset [Kersey et al., 2004] and those of a locally curated dataset containing primate proteins and common protein contaminants and artefacts. SEQUEST was used with the "no enzyme" option and specifying methionine and tryptophan oxidations as potential modifications. The first-pass search results were validated as follows: (a) peptide assignments with a PeptideProphet probability $\geq$90% were accepted; (b) peptide assignments with a probability $<$50% were rejected; (c) peptide assignments with a probability in-between 50% and 90% were accepted or rejected by an expert mass spectrometrist after verification of the corresponding MS/MS spectra. Notwithstanding rule (a), when a protein was identified by less than four peptides having a probability $\geq$50%, all of its peptides were manually verified. For the second pass, MS/MS spectra were searched against a subset database consisting of all the proteins identified by the first pass, including any splice isoforms or gene variants similar to those proteins (as indicated by ProteinProphet). SEQUEST was used with the "trypsin (KR/P)" option and specifying methionine and tryptophan oxidations as well as arginine and lysine methylation, dimethylation, trimethylation, and acetylation as potential modifications. The second-pass search results were validated as follows: (a) peptide assignments with an second-pass X_{Corr} value lower than the first-pass X_{Corr} value obtained for the corresponding MS/MS spectrum were rejected; (b) remaining peptide assignments with a probability $<$80% were rejected; (c) remaining peptide assignments with a probability $\geq$80% were accepted or rejected by an expert mass spectrometrist after verification of the corresponding MS/MS spectra. The application of the above-described validation protocol yielded thorough and rigorous peptide fragmentation fingerprinting identifications, and ensured that only proteins identified with high confidence are reported in this study.

RESULTS

Relative Expression of Two Human PARP-3 Isoforms

The recent characterization of the human *parp-3* gene (*ADPRTL3*) revealed the possible existence of two different human PARP-3 isoforms owing to the presence of two splicing acceptor sites in exon 3 [Urbanek et al., 2002] (Fig. 1A). The use of the splicing acceptor site E3a produces transcripts (transcripts 2 and 3, Fig. 1A) encoding the previously described 533 amino acid PARP-3 (short isoform: hPARP-3_{short}, Fig. 1B) [Johansson, 1999]. The use of the splicing acceptor site E3b produces transcript 1. In transcript 1, an ATG start codon from exon 1 is in-frame with the ATG start codon in exon 3 (see transcript 1, Fig. 1C), separated by 6 codons. Therefore, transcript 1 encodes a long PARP-3 variant (hPARP-3_{long}) that has an extension of 7 amino acids at the N-terminus relative to hPARP-3_{short} (Fig. 1B,C) [Augustin et al., 2003]. The predicted molecular weight of hPARP-3_{long} (60,952 Da) is thus slightly larger than that of hPARP-3_{short} (60,116 Da). To determine the relative frequency of use of each acceptor site in exon 3 and thus evaluate the relative abundance of each alternatively spliced transcript, the GenBank human expressed sequence tag (EST) database (January 17, 2005) was searched for sequences matching 160 nucleotides spanning the exon 1-exon 3 boundary using the NCBI BLAST program. Thirty-one ESTs were found sharing sequence identity with the query sequence. Splice variants formed by using the E3b acceptor site accounted for 23% (7) of ESTs (transcript 1, Fig. 1A,C). We identified two different transcripts spliced at the E3a acceptor

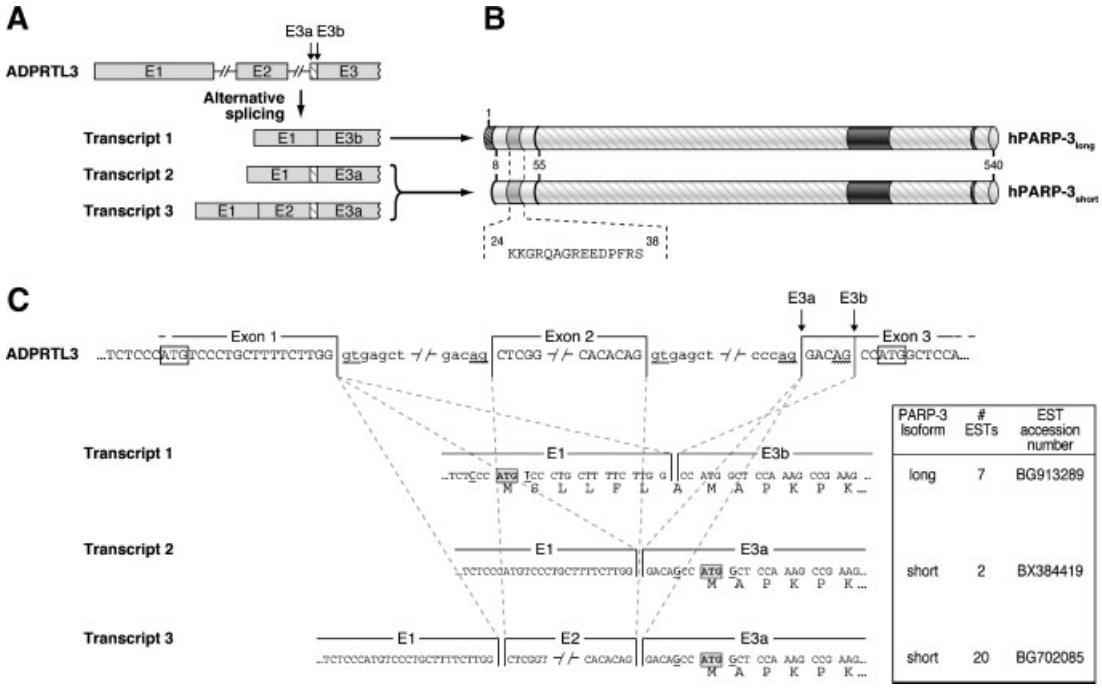

Fig. 1. The human PARP-3 gene (ADPRTL3) is alternatively spliced to encode two PARP-3 isoforms, hPARP-3_{short} and hPARP-3_{long}. **A**: Schematic representation of the first 3 exons of human ADPRTL3 gene and transcripts generated by alternative splicing. Expression of ADPRTL3 produces three different transcripts due to alternative splicing of exon 1 (E1) and 2 (E2) and the presence of two adjacent acceptor sites in exon 3 (E3a and E3b). Despite several possible alternative splicing combinations, only transcripts 1–3 are produced, as surveyed in human EST databases (see text). **B**: Schematic representation of the two hPARP-3 splice variants encoded by transcripts 1–3. hPARP-3_{long}, encoded by transcript 1, has a N-terminal 7 amino acid extension (dark hatched region) that is absent from hPARP-3_{short}, encoded by transcripts 2 and 3. Amino acid coordinates shown are those of hPARP-3_{long}. In the C-terminal domain (amino acids 55–540), dark gray zones correspond to the PARP signature region. The peptide used to generate anti-PARP-3 antibodies (amino acids 24–38) is shown below protein structures. **C**: Sequence details of ADPRTL3 and transcripts. Upper line: Segments of ADPRTL3 genomic sequence are shown with splice donor (gt) and acceptor (ag) sites in the first three exons/introns. Intron and exon sequences are in lower and upper case, respectively. ATG corresponding to start codons are boxed. Lower lines: Transcript 1 is formed by splicing of exon 1 with exon 3 at the E3b acceptor site and encodes hPARP-3_{long}. hPARP-3_{short}, encoded by transcripts 2 and 3 spliced at the E3a site, lacks the first 7 amino acids of the long isoform. The N-terminal amino acid sequence of each PARP-3 isoform is shown below the transcript nucleotide sequences. According to the −3 and +4 nucleotide positions relative to ATG start codons (underlined in transcript sequences), ATG of the long isoform is in a weak context while that of the short isoform is strong (see text) [Kozak, 1989, 1995]. The box on the right specifies the number of human expressed sequence tags (ESTs) in the NCBI database (as of January 17, 2005) corresponding to each transcript and the accession number of an EST matching each sequence as an example. Accession numbers for ADPRTL3 and PARP-3 are NM_005485 and Q9Y6F1 respectively.

site (transcripts 2 and 3, Fig. 1A,C). Transcript 2 (2 ESTs) and transcript 3 (20 ESTs), that differ by the alternative splicing of exon 2, together represent 71% of ESTs (Fig. 1C). Finally, two ESTs out of the 31 identified contained intronic sequences and are thus not represented. The existence of these three transcripts suggests that both PARP-3 isoforms are expressed in human cells. However, the preferential use of the E3a splicing acceptor site (71%) suggests that hPARP-3_{short} may be more abundant than hPARP-3_{long}. Interestingly, none of the ESTs spliced at the E3b site comprised exon 2. Such a transcript would have encoded a very short protein unrelated to hPARP-3 besides starting with the MSLLFLA sequence of the long isoform because of an in-frame stop codon in exon 2. This indicates that the hPARP-3 ESTs are representative of coding transcripts and not of immature ones.

Furthermore, from a detailed analysis of the nucleotide sequence of hPARP-3 ESTs, we noticed that the start codon of hPARP-3_{long} coding sequence ($\mathbf{C}^{-3}$CCATG$\mathbf{T}^{+4}$) is in a weak context while the start codon of hPARP-3_{short} coding sequence is in a strong context ($\mathbf{G}^{-3}$ CCATG$\mathbf{G}^{+4}$) (strong start sites have $(\mathbf{A}/\mathbf{G})^{-3}$ XXATG$\mathbf{G}^{+4}$ [Kozak, 1989, 1995]; Fig. 1C). This

raises the possibility that initiation of translation could occur at both ATGs in transcript 1, again favoring the expression of hPARP-3_{short} [Kozak, 1995]. Therefore, in contrast to a previous report suggesting that only hPARP-3_{long} is expressed in human cells [Augustin et al., 2003], our analysis of hPARP-3 ESTs rather indicates that both splice isoforms are expressed and suggests that the expression of hPARP-3_{short} is favored. Of note, a single splicing acceptor site (equivalent to E3a) is present in the corresponding exon of the mouse *parp-3* ortholog, and therefore, a unique parp-3, homologous to hPARP-3_{short}, is expressed in mouse [Urbanek et al., 2002].

Subcellular Distribution of PARP-3

We monitored the distribution of PARP-3 isoforms by transiently expressing hPARP-3_{short} and hPARP-3_{long} in COS-7 and HeLa cell lines. hPARP-3_{short} and hPARP-3_{long} tagged on the N-terminal side with green fluorescent protein (GFP-hPARP-3_{short} and GFP-hPARP-3_{long}) are mostly nuclear in HeLa and COS-7 cells (Fig. 2A). No significant difference between the distribution of long and short isoforms are observed (Fig. 2A). A similar distribution was seen for FLAG-tagged hPARP-3 isoforms in HeLa and COS-7 cells (not shown). From these observations, we conclude that hPARP-3 is predominantly nuclear and that the seven amino acid extension in hPARP-3_{long} is not responsible for a specific subcellular targeting.

To examine the cellular distribution of endogenous PARP-3, we generated a polyclonal antiserum directed against a peptide corresponding to amino acids 24–38, a region lacking sequence similarity with any of the other known PARPs but common to hPARP-3_{long} and hPARP-3_{short} (Fig. 1B). To verify the specificity of this antiserum for PARP-3, FLAG-tagged PARP-1, PARP-2, and PARP-3 were transiently expressed in COS-7 (PARP-1) or HeLa cells (PARP-2 and PARP-3) and whole cell extracts were analyzed by Western blotting. Immunodetection with the anti-FLAG antibody M2 confirmed the expression of the three FLAG-tagged PARPs (Fig. 3A, lanes 1–3). The PARP-3 antiserum specifically detected FLAG-hPARP-3 by Western blot and not PARP-1 or PARP-2 (Fig. 3A, lanes 4–6). A faint band detected at 62 kDa in lane 4 is endogenous PARP-3 detected in this extract prepared from COS-7 cells. The preimmune serum does not react with any of the expressed PARPs (Fig. 3A, lanes 7–9).

We also evaluated the anti-PARP-3 antibody for immunodetection of hPARP-3 by immunofluorescence. Using the anti-PARP-3 antibody, we verified that the staining pattern observed for GFP-hPARP-3_{short} in transfected cells matches that produced by anti-PARP-3 in the same cells (Fig. 3B). Again, the preimmune serum did not detect GFP-PARP-3 or any other cellular component (Fig. 3B).

The subcellular distribution of endogenous PARP-3 was examined in exponentially growing HeLa and COS-7 cells with the PARP-3 antiserum. Immunostaining of these cells indicates that the endogenous protein is predominantly nuclear, as observed for the transiently expressed tagged PARP-3 (Fig. 2B; Left panels of Fig. 4A–C and of Fig. 5A,B). Some cytoplasmic staining is detected, being slightly more important in HeLa than COS-7 cells (Fig. 2B). These results thus confirm the predominantly nuclear distribution of PARP-3 observed for the transiently expressed tagged hPARP-3 isoforms.

In a previous publication, hPARP-3_{long} was reported to be exclusively centrosomal owing to the extension of 7 amino acids at its N-terminus [Augustin et al., 2003]. We monitored the co-localization of GFP-tagged hPARP-3_{long} and hPARP-3_{short} with γ-tubulin, a centrosomal marker, in HeLa cells. Although we could see on very rare occasions some co-localization of GFP-hPARP-3 (either long or short) with γ-tubulin, we did not observe the unique centrosomal localization for GFP-hPARP-3_{long} previously reported (not shown). Using our anti-PARP-3 antibody, we also monitored localization of endogenous PARP-3 in centrosomes using transiently expressed GFP-centrin, pericentrin and ninein as centrosomal markers [Ou et al., 2002] (Fig. 4A–C). However, we found no significant co-localization of PARP-3 with the centrosomal markers. We could detect some PARP-3, in about 5% of centrosomes, only if overexposed pictures were taken.

PARP-3 Co-Localizes With Polycomb Group Bodies

The nuclear staining pattern of endogenous PARP-3 is punctate rather than uniform. In each cell, numerous small nuclear foci are detected, as well as a few larger foci (Fig. 2B; see also left panels in Fig. 4A–C and Fig. 5A,B).

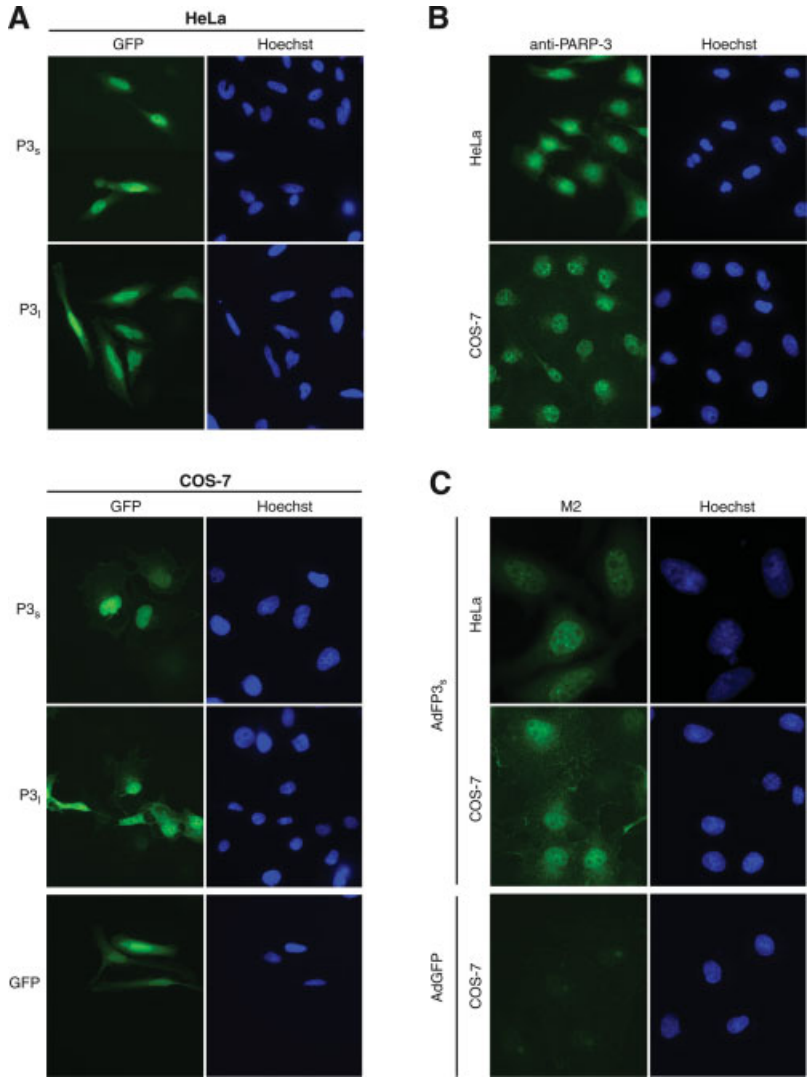

Fig. 2. Subcellular distribution of PARP-3. **A**: The short and long PARP-3 isoforms tagged with GFP accumulate predominantly in the nucleus of HeLa and COS-7 cells. Cells grown on coverslips were transfected with pGFP-hPARP-3_{short} ($P3_s$), pGFP-hPARP-3_{long} ($P3_l$), or pEGFP-C1 empty vector (GFP, bottom left) fixed and DNA was stained with Hoechst 33342. **B**: Endogenous PARP-3 is mostly nuclear in HeLa and COS-7 cells. PARP-3 was immunostained with polyclonal anti-PARP-3 antibodies (see Fig. 3) and DNA was counterstained with Hoechst 33342. **C**: FLAG-tagged PARP-3 is mostly nuclear. HeLa and COS-7 cells were infected with the recombinant adenovirus $AdFP3_s$ to express FLAG-tagged hPARP-3_{short} or with the control recombinant adenovirus AdGFP. Distribution of FLAG-hPARP-3_{short} was detected with the anti-FLAG antibody M2. [Color figure can be viewed in the online issue, which is available at www.interscience.wiley.com.]

This punctate staining was not seen for GFP-PARP-3 or FLAG-PARP-3 in transfected cells, most likely because they are overexpressed. However, this punctate distribution is clearly detected for FLAG-hPARP-3_{short} transiently expressed at low levels after infections with 10 pfu/cell (10 MOI) of the recombinant adenovirus ADFP3 expressing FLAG-hPARP-3_{short} (Fig. 2C; see also Fig. 5C, left panel). The larger nuclear foci decorated by the anti-PARP-3 antibodies are reminiscent of Polycomb group (PcG) bodies. These PcG bodies are unique nuclear structures in regions of pericentric heterochromatin. These regions are sites of specific trimethylation of histone H3 on lysine residue 27 (tmK27) by the polycomb group protein EZH2. PcG proteins, that include EED, YY1, RbAp46/48, and Suz12, are required for transcriptional silencing of specific target loci. To evaluate the possible localization of PARP-3 at PcG bodies, we assessed its staining pattern relative to that of PcG proteins by immunofluorescence microscopy. We monitored PARP-3 distribution relative to that of tmK27,

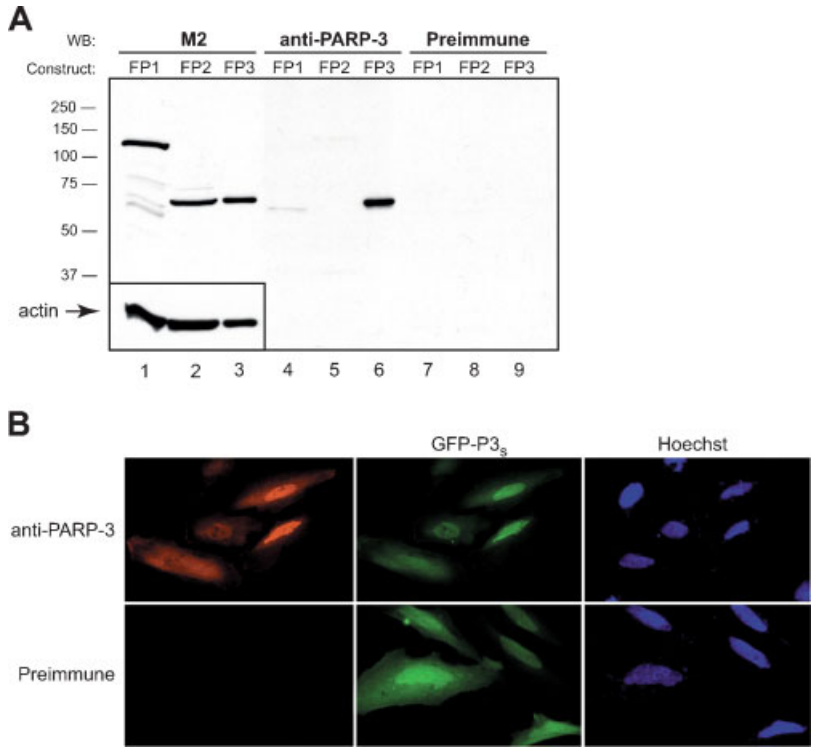

Fig. 3. Characterization of the polyclonal anti-PARP-3 antibodies. **A**: Western blot analysis of anti-PARP-3 antibodies. FLAG-tagged PARP-1 (FP1), PARP-2 (FP2), and PARP-3 (FP3) transiently expressed in COS-7 (PARP-1) or HeLa (PARP-2 and PARP-3) cells were detected with anti-FLAG antibody M2 (**lanes 1–3**). The anti-PARP-3 antibodies detected PARP-3 (**lane 6**) but not PARP-1 or PARP-2 (**lanes 4** and **5**). The faint band detected in lane 4 at about 62 kDa is endogenous PARP-3 which is more abundant in COS-7 than HeLa cells. The preimmune serum does not detect PARP-1, PARP-2, or PARP-3 (**lanes 7–9**). **B**: HeLa cells grown on coverslips were transfected with pGFP-hPARP-3_{short}, fixed and PARP-3 was detected with anti-PARP-3 antibodies or preimmune serum. The staining pattern produced by anti-PARP-3 and GFP-PARP-3 is nearly identical, demonstrating the specificity of anti-PARP-3. The preimmune serum does not stain GFP-PARP-3_{short} or any other cellular component. [Color figure can be viewed in the online issue, which is available at www.interscience.wiley.com.]

RbAp46/48, and YY1 (Fig. 5). These experiments were conducted both in COS-7 and HeLa cells and produced similar observations. tmK27 is specifically found in PcG bodies, resulting from EZH2 activity. We indeed found co-localization of PARP-3 large nuclear foci with tmK27, while small PARP-3 nuclear foci are not sites of tmK27 staining (Fig. 5B). Similarly, the large nuclear foci stained by anti-PARP-3 matched remarkably well with the RbAp46/48 distribution (Fig. 5A). To permit co-localization of PARP-3 with YY1 (for which a polyclonal antibody was available), HeLa cells expressing low levels of FLAG-PARP-3_{short} after AdFP3 infection were used. FLAG-PARP-3_{short} partially co-localizes with YY1, in regions of large nuclear foci (Fig. 5C). This indicates that only the subpopulation of PARP-3 detected in the large nuclear foci co-localizes with PcG proteins while there is little if any co-localization between small PARP-3 nuclear foci and the PcG proteins YY1 and RbAp46/48.

Polycomb Group Proteins Form a Complex With hPARP-3

To characterize further the interaction of PARP-3 with proteins of PcG bodies, we conducted immunoprecipitations of FLAG-hPARP-3_{short} expressed at moderate levels after infections of HeLa and COS-7 cells with 10 MOI of the recombinant adenovirus AdFP3 (see Materials and Methods). AdGFP, a recombinant adenovirus that drives the expression of GFP, was used to infect control cells. FLAG-hPARP-3_{short} was immunoprecipitated under mild conditions using the antibody M2 which specifically binds the FLAG epitope. Magnetic beads conjugated to protein G were used to capture complexes. Immunoprecipitated complexes were eluted from magnetic beads by boiling in reducing sample buffer and analyzed by Western blotting with a panel of antibodies against PcG proteins. We detected several PcG proteins in the immunoprecipitated complexes, namely

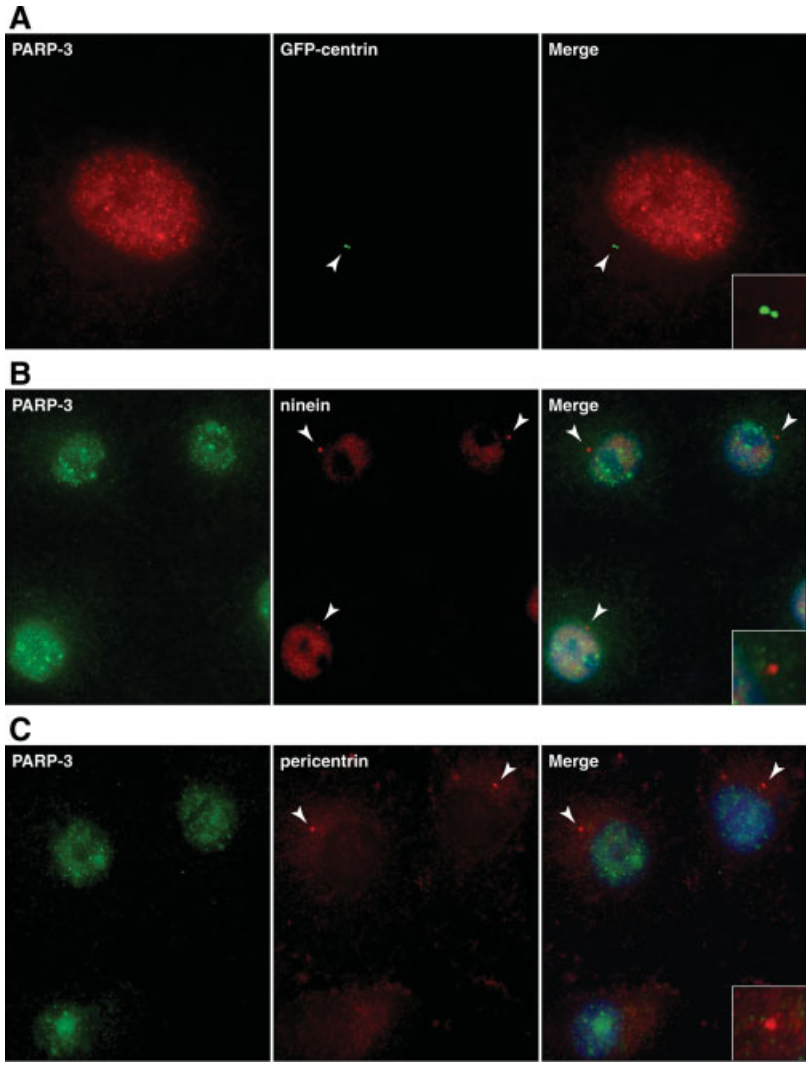

Fig. 4. Centrosomes contain minute amounts of PARP-3. **A**: COS-7 cells were transfected with GFP-BBS6 to express GFP-tagged centrin. Cells were fixed and immunostained with anti-PARP-3. Arrows indicate the centrosome, where GFP-centrin accumulates. **B**: COS-7 cells were fixed and dually immunostained for the centrosomal marker ninein and for PARP-3. **C**: COS-7 cells were fixed and immunostained for the centrosomal marker pericentrin and for PARP-3. Arrowheads indicate centrosomes. B, C: specific antibodies against endogenous proteins were used (see Materials and Methods). Merged images (B) and (C) include DAPI staining. Magnifications in the centrosomal area are shown in the lower right corner of merged images. [Color figure can be viewed in the online issue, which is available at www.interscience.wiley.com.]

EZH2, Suz12, and YY1, confirming the interaction of PARP-3 with PcG bodies (Fig. 6). We also detected hdac1 and hdac2, two histone deacetylases involved in PcG-dependent transcriptional repression (Fig. 5). Taken together, microscopy and biochemical data strongly support an interaction of PARP-3 with PcG bodies.

Identification of Other hPARP-3 Protein Partners by Mass Spectrometry

A proteomics approach was undertaken to identify other proteins that interact with PARP-3 in vivo. FLAG-hPARP-3_{short} or FLAG-hPARP-3_{long} transiently expressed in COS-7 cells by transfection of the corresponding plasmid constructs were immunoprecipitated in mild conditions as described above. FLAG-hPARP-3 and its binding partners were then specifically eluted from the M2-magnetic bead support using the FLAG peptide. Eluted proteins were separated by SDS–PAGE and the gel was stained with Sypro Ruby. Proteins immunoprecipitated with FLAG-hPARP-3_{short} are shown in Figure 7. An identical protein pattern was obtained after immunoprecipitation of

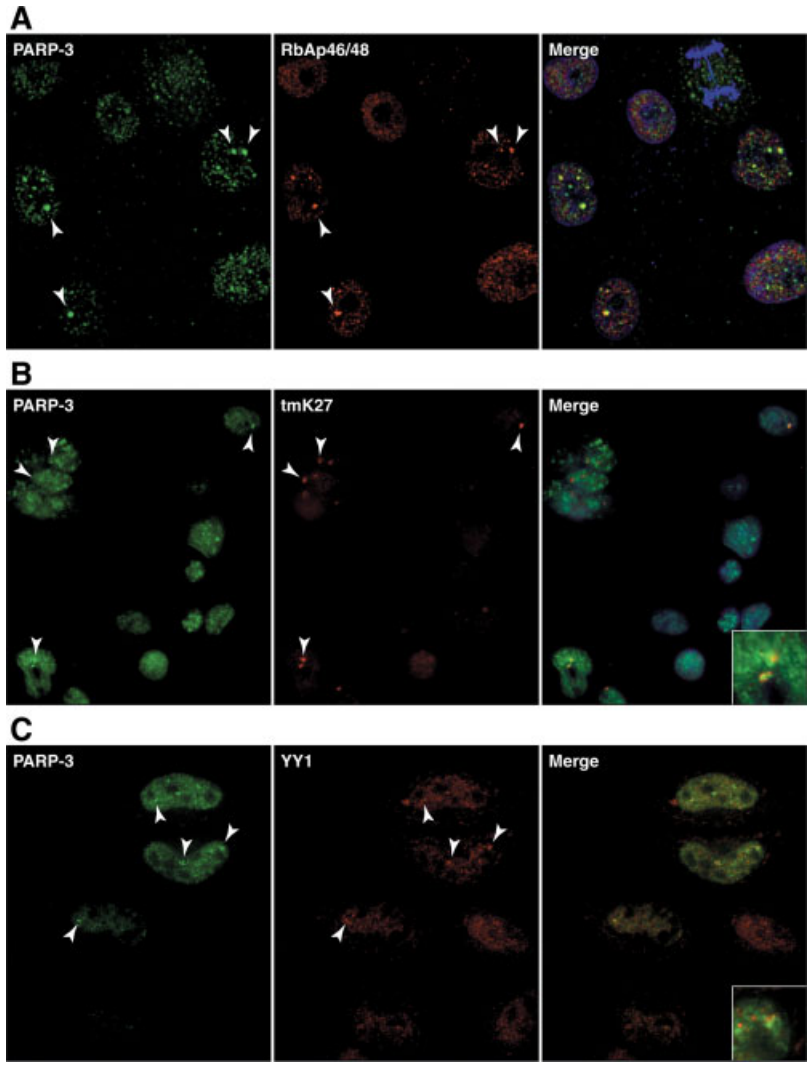

Fig. 5. PARP-3 is a component of Polycomb group bodies. COS-7 cells were fixed and dually immunostained with anti-PARP-3 and (**A**) anti-RbAp46/48 or (**B**) with anti-histone H3 trimethylated on K27 residue (tmK27). **C**: HeLa cells infected with 10 MOI AdFP3 were fixed and dually stained with M2 to detect FLAG-PARP-3_{short} and anti-YY1. Arrowheads indicate PcG bodies. Merged images (A) and (B) include DAPI staining. Magnifications of PcG bodies are shown in the lower right corner of the merged images. [Color figure can be viewed in the online issue, which is available at www.interscience.wiley.com.]

FLAG-hPARP-3_{long} (not shown). We repeatedly detected six protein bands that were excised from the gel, digested with trypsin and analyzed by LC-MS/MS (Fig. 7). The catalytic subunit of DNA-dependent protein kinase (DNA-PKcs), PARP-1, DNA ligase III, DNA ligase IV, Ku80, and Ku70 were identified with high confidence as proteins co-immunoprecipitated with FLAG-hPARP-3_{short} and FLAG-hPARP-3_{long} (Table I; Supplemental Table I). Estimated molecular weight of proteins identified by LC-MS/MS corresponded well with electrophoretic mobility of proteins immunoprecipitated with FLAG-PARP-3 (Table I and Fig. 7). Among peptides matching with DNA-PKcs sequence, two corresponded to a sequence unique to the splice variant 1, thus specifying that this variant of DNA-PKcs is present in the sample. In constrast, peptides detected for DNA ligase III did not permit the discrimination between α or β isoforms (Table I; see also supplemental Table I for a list of identified peptides).

Next, we confirmed spectrometric identifications of DNA-PKcs, Ku80, Ku70, and PARP-1 by Western blot analysis of complexes immunopurified with both isoforms of FLAG-hPARP-3 (Fig. 8A). These same proteins were also detected after immunoprecipitations conducted

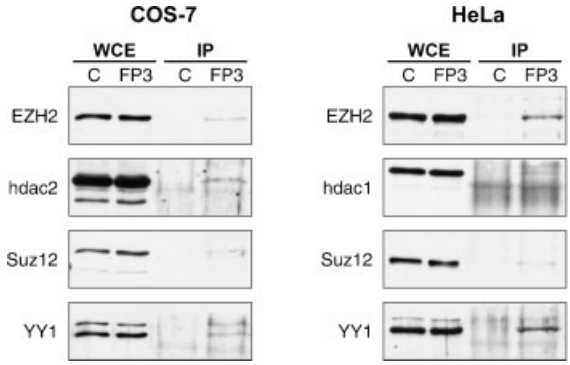

Fig. 6. PARP-3 interacts with Polycomb group proteins. COS-7 or HeLa cells were infected with AdFP3 (lanes FP3) or the control adenovirus AdGFP (lanes C). Cell lysates were prepared 24 h post-infection and FLAG-PARP-3_{short} was immunoprecipitated in mild conditions to preserve protein–protein interactions using the FLAG-specific antibody M2. Cell lysates (WCE, 10% of input) and immunoprecipitated proteins (IP) were separated by SDS–PAGE and immunoblotted with the indicated antibodies (left of panels) against Polycomb group proteins.

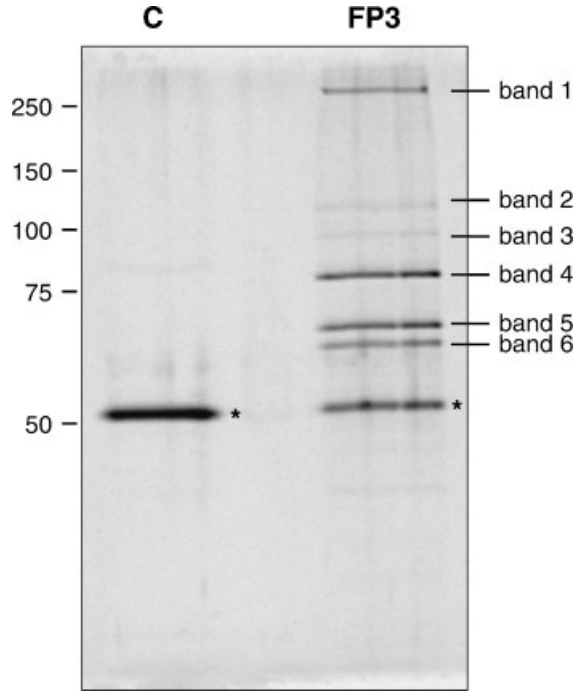

Fig. 7. Proteins immunopurified with FLAG-hPARP-3_{short}. **A**: Cell lysates prepared from COS-7 cells transiently expressing FLAG-hPARP-3_{short} (lane FP3) or not (lane C) were incubated with the antibody M2 and magnetic beads coupled to protein G to immunocapture FLAG-hPARP-3_{short} and interacting partners. After extensive washes of beads, immunoprecipitated proteins were specifically eluted by incubation with FLAG peptides. Eluted proteins were separated on an 8% SDS–polyacrylamide gel and revealed by staining with Sypro Ruby. Indicated protein bands were excised from the gel and digested with trypsin. LC-MS/MS analysis was conducted to identify protein partners. Bands labeled with an asterisk correspond to the heavy chain of M2 used in the immunoprecipitation.

in HeLa cells (Fig. 8A). A reverse pull-down was also conducted with myc-tagged Ku70 to verify the specificity of the interaction with PARP-3. Myc-tagged Ku70 was immunoprecipitated from COS-7 cells co-expressing FLAG-hPARP-3_{short}. Proteins interacting with myc-Ku70 were detected by Western blotting (Fig. 8B). As expected, FLAG-hPARP-3_{short} was pulled-down by myc-Ku70, as well as Ku80, DNA-PKcs, and PARP-1. We concluded that this proteomics approach allowed the identification of the major partners of PARP-3. The detection limit of Sypro Ruby Red used to stain immunoprecipitated proteins is approximately 50–100 fmol (3–6 ng) for a 60 kDa protein. Thus less abundant proteins and proteins interacting with a small subset of PARP-3, such as PcG proteins, were not detected by this approach.

Because Sypro Ruby stain is quantitative for a linear range of three orders of magnitudes, we can evaluate the relative amount of the proteins immunoprecipitated with PARP-3. Intensities of Sypro-stained protein bands indicate that Ku70 and Ku80 are the most abundant proteins immunoprecipitated with FLAG-hPARP-3 and suggest that the three proteins are recovered at an apparent 1:1:1 stochiometry (Fig. 7, bands 4–6). In contrast, DNA-PKcs, PARP-1, and DNA ligase III/IV are far less abundant (Fig. 7, compare bands 1–3 with band 6). This suggests that the interactions of FLAG-hPARP-3_{short} with Ku70 and Ku80 are not solely mediated by PARP-1, known to interact with these proteins, nor by DNA-PKcs, which forms the DNA-PK complex with Ku70 and Ku80 in response to DNA double-strand breaks.

Because all of the identified protein partners are DNA-binding proteins and PARP-3 may have some DNA binding activity [Augustin et al., 2003], FLAG-hPARP-3 could be interacting with the identified proteins by binding to common DNA regions. We tested the effect of a nuclease treatment on the composition of the immunoprecipitated FLAG-hPARP-3_{short} complexes. This was monitored by Western blot analysis. Treatment of the whole cell extract with Benzonase® prior to immunoprecipitation caused the release of Ku70 and Ku80 from complexes, while DNA-PKcs and PARP-1 remained associated with FLAG-hPARP-3_{short} (Fig. 9). These results are consistent with interactions between FLAG-hPARP-3 and

TABLE I. List of Proteins Immunoprecipitated with FLAG-hPARP-3 Identified by LC-MS/MS[a] (see Fig. 7)

Band	Protein name	MW[b] (kDa)	SwissProt accession no.	International Protein Index[c]	PARP-3_{short}			PARP-3_{long}		
					Sequence coverage (%)	Unique matching peptides	Total number matching peptides	Sequence coverage (%)	Unique matching peptides	Total number matching peptides
1	DNA-PKcs	469	P78527	IPI00296337	10	43	112	14	65	159
2	PARP-1	113	P09874	IPI00292802	8.4	7	10	12	10	15
3	DNA ligase III	103	P49916	IPI00000156	5.5	4	4	15	13	16
				IPI00029081						
3	DNA ligase IV	104	P49917	IPI00217669	0.9	1	1	3.7	3	3
4	Ku80	83	P13010	IPI00220834	24	21	44	23	18	27
5	Ku70	70	P12956	IPI00395343	29	26	40	16.6	10	13
6	PARP-3	63[d]	Q9Y6F1	IPI00023184	22	15	23	23	14	26
				IPI00333507						

[a]See Supplemental Table I for the list of identified peptides.
[b]Estimated molecular weight of human proteins.
[c]Kersey et al. [2004].
[d]Molecular weight of FLAG-hPARP-3.

Ku70/Ku80 mediated by DNA while that with DNA-PKcs and PARP-1 are independent of DNA.

DISCUSSION

The cellular and biochemical characteristics of human PARP-3 described in this report reveal that PARP-3 resides predominantly in the nucleus of mammalian cells, with minor cytoplasmic accumulation in some cells. We find that the 7 amino acid extension of PARP-3_{long} does not target it to a specific subcellular location because the distribution of both PARP-3 isoforms, either GFP or FLAG-tagged, is similar. Taken together, the similar subcellular distribution of transiently expressed and endogenous PARP-3 and our analysis of the relative abundance of PARP-3 transcripts and context of the initiation codons all suggest that both isoforms are expressed in mammalian cells. Furthermore, despite our attempts to monitor PARP-3 in centrosomes, we could not confirm the previously reported exclusive expression of the long isoform as well as the accumulation of the transiently expressed long isoform in centrosomes [Augustin et al., 2003]. We detected a very small fraction of endogenous PARP-3 in centrosomes in no more than 5% of cells.

Immunofluorescent analysis of the subcellular distribution of PARP-3 revealed a widespread localization in small nuclear foci. In addition, PARP-3 accumulates in a small number of larger foci that co-localize with PcG bodies. In mammalian cells, these bodies appear in defined areas of the nucleus, the larger bodies being generally localized near centromeres [Saurin et al., 1998]. They consist of Polycomb group proteins assembled in chromatin-associated multiprotein complexes. These well conserved PcG proteins cooperate to maintain specific gene silencing essential for development and proper cell type functions in an organism. Biochemical studies indicate that PcG proteins associate in two general classes of Polycomb repressive complexes (PRCs) [Levine et al., 2004]. The current model of PRC functions suggests that class I complexes are responsible for maintenance of repression through posttranslational modification while class II complexes are recruited by class I to directly inhibit gene expression. The core class I PcG complexes (PRC2 and PRC3) comprise

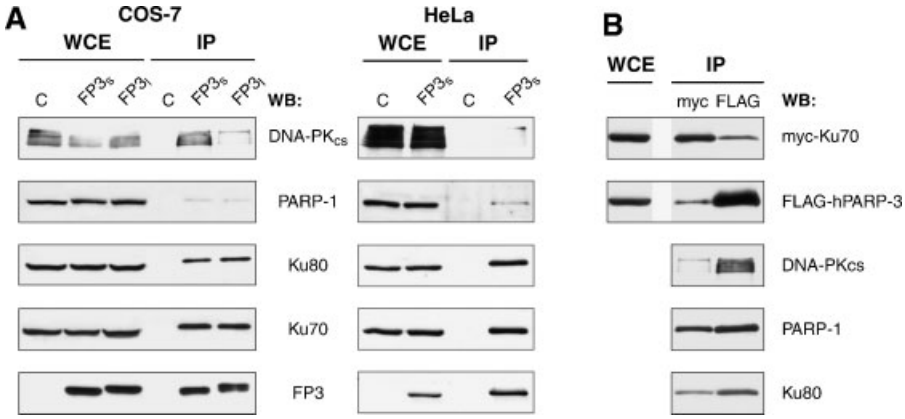

Fig. 8. Western blot analysis of FLAG-hPARP-3 protein partners. **A**: hPARP-3 short and long isoforms interact with the same partners. Cell extracts (WCE) were prepared from COS-7 or HeLa cells transfected with pFLAG-hPARP-3_{short} ($FP3_s$) or pFLAG-hPARP-3_{long} ($FP3_l$). Proteins immunoprecipitated (IP) with M2 were analyzed by Western blotting. The control (C) lane shows proteins immunoprecipitated from cells that do not express a FLAG-tagged protein. **B**: Immunoprecipitation of myc-Ku70 pulls down FLAG-hPARP-3_{short} and partners. Immunoprecipitation was carried out from lysates of COS-7 cells co-expressing myc-Ku70 and FLAG-hPARP-3_{short} using either anti-myc or M2 antibodies, as indicated above lanes. A, B: Immunoprecipitated proteins were detected by westerblot with indicated antibodies. Whole cell extracts (WCE) shown correspond to 10% of the lysates used for immunoprecipitations.

the histone methyltransferase EZH2, Suz12, RbAp46/48, and EED. The specific methylation of K27 residue of histone H3 by EZH2 is believed to mark genetic regions for silencing carried out by the PRC1 complex comprising BMI-1, RING1, and HPC proteins. A number of other proteins associate with the core PRC complexes and are thought to modulate their functions. This includes the histone deacetylases HDAC1 and HDAC2 and the transcription factor YY1 [Chang et al., 2001; Atchison et al., 2003]. With the currently available anti-PcG antibodies, we have identified PARP-3 in association with several PcG proteins of the PRC2/3 complex, including the methyltransferase EZH2 and Suz12. This suggests that a further level of regulation of silencing could be provided by PARP-3-dependent poly(ADP-ribosyl)ation. The current cellular targets of PARP-3 are unknown, but could include proteins of the PRC2/3 complex with which PARP-3 interacts, or histones at sites of PcG-dependent silencing. Regulation of chromatin structure by PARP-1-dependent poly(ADP-ribosyl)ation has been long known to play a key role in maintenance of genomic integrity and more recently in transcriptional regulation [reviewed by D'Amours et al., 1999; Tulin and Spradling, 2003; Rouleau et al., 2004]. PARP-3 may have a parallel function that specifically targets sites of PcG-dependent silencing.

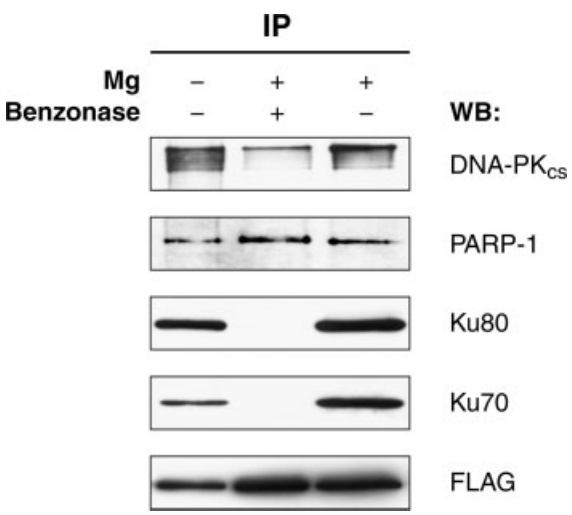

Fig. 9. The interactions of FLAG-hPARP-3_{short} with Ku70 and Ku80 are dependent on nucleic acids. $MgCl_2$ (1 mM) was added to whole cell lysates of COS-7 cells expressing FLAG-hPARP-3_{short}. Lysates were incubated with or without 25 U Benzonase®. Immunoprecipitation of FLAG-hPARP-3_{short} and interacting proteins was subsequently carried out. Immunoprecipitated proteins were detected by Western blot analysis using antibodies against indicated proteins.

By affinity purification and proteomics identification, we have identified the major protein partners of PARP-3. These interactors are essentially nuclear, supporting the microscopic observation that PARP-3 is found mostly in the nucleus of COS-7 and HeLa cells. Moreover, our results indicating that both splice variants of hPARP-3 immunoprecipitated the same protein

partners further support our fluorescence microscopy observations that they have similar subcellular distributions and that they could function in similar protein complexes. It is striking that the major protein partners of PARP-3 are all involved with DNA damage signaling and/or repair, suggesting that PARP-3 is also part of this network. Ku70, Ku80 and DNA-PKcs form the DNA-PK complex responsible for the repair of double strand breaks by non-homologous end joining (NHEJ). NHEJ also requires the activity of XRCC4 and DNA ligase IV. The detection of DNA ligase IV by mass spectrometric analysis of PARP-3 complexes is therefore consistent with an involvement of PARP-3 in NHEJ. Indeed, evidence is accumulating that inhibition of PARP activity results in altered efficiency of NHEJ reactions by DNA-PK [Audebert et al., 2004; Veuger et al., 2004].

PARP-1 and PARP-2 are important players of DNA single-strand break repair by base excision. Through synthesis of poly(ADP-ribose), they recruit XRCC1 and DNA ligase III which participate in the base excision repair (BER) process with DNA polymerase β [Leppard et al., 2003]. Thus, the identification of PARP-1 and DNA ligase III immunoprecipitated with PARP-3 also links PARP-3 to a role in BER. PARP-2 was not identified in immunoprecipitated proteins by LC-MS/MS and Western blotting. However, we cannot exclude it as a partner of PARP-3. It may have escaped detection due to its low abundance in isolated FLAG-hPARP-3 complexes and anti-PARP-2 antibodies currently available may lack suitable sensitivity.

Several PARP-3 protein partners identified are known to also interact with PARP-1. These include DNA-PKcs, Ku70/Ku80, DNA ligase III, and the transcription factor YY1 [Ruscetti et al., 1998; Galande and Kohwi-Shigematsu, 1999; Oei and Shi, 2001; Li et al., 2004]. This suggests that PARP-3, as it is the case for PARP-2, could have some functional redundancy with PARP-1. However, because the activity of PARP-3 is not activated by DNA strand breaks and is far less processive than PARP-1 [Augustin et al., 2003], it is most likely that PARP-3 has specific functions that could be fulfilled in distinct cellular contexts apart from those involving PARP-1. It is now generally well accepted that PARP-1 regulates transcription not only by modulating chromatin structure but also by interacting and modifying the activity of several transcription factors including YY1, NFκB, and RNA polymerase II [Matsui et al., 1980; Oei et al., 1998; Hassa et al., 2003]. Conversely, activation of PARP-1 and DNA repair by YY1 has also been reported [Oei and Shi, 2001], leading to the proposal that PARP-1 could act as a regulatory switch that represses transcription to allow DNA repair when damage occurs [Ziegler and Oei, 2001]. Furthermore, Ku70 and Ku80 functionally interact with YY1 to repress myosin heavy chain gene expression and Ku80 significantly contributes to the efficiency of transcriptional reinitiation [Woodard et al., 2001; Sucharov et al., 2004]. These observations support the existence of cross-talk between gene expression and DNA repair pathways. PARP-3 may also be involved in this cross-talk.

ACKNOWLEDGMENTS

We thank Dr. S. Lees-Miller for anti-Ku70 antibodies, M.-E. Bonicalzi for helpful discussions and members of the Poirier lab for critical reading of the manuscript. The GFP-BBS6 construct was a kind gift from Dr. J.B. Rattner (University of Calgary). Pericentrin and ninein antibodies were kindly provided by Dr. G. Chan (University of Alberta). Authors also wish to acknowledge the excellent work of the Infography group of the CHUL research center. This work was supported by operating grants from the Canadian Institutes for Health Research. G.G.P. holds a Canada Research Chair in Proteomics. C.P. is financed by the Ligue Nationale Contre le Cancer (équipe labellisée).

REFERENCES

Alvarez-Gonzalez R, Althaus FR. 1989. Poly(ADP-ribose) catabolism in mammalian cells exposed to DNA-damaging agents. Mutat Res 218:67–74.

Amé JC, Rolli V, Schreiber V, Niedergang C, Apiou P, Decker P, Muller S, Hoger T, Ménissier-de Murcia J, de Murcia G. 1999. PARP-2: A novel mammalian DNA damage dependent poly(ADP-ribose) polymerase. J Biol Chem 274:17860–17868.

Amé JC, Spenlehauer C, de Murcia G. 2004. The PARP superfamily. Bioessays 26:882–893.

Atchison L, Ghias A, Wilkinson F, Bonini N, Atchison ML. 2003. Transcription factor YY1 functions as a PcG protein *in vivo*. EMBO J 6:1347–1358.

Audebert M, Salles B, Calsou P. 2004. Involvement of PARP-1 and XRCC1/DNA ligase III in an alternative route for DNA double-strand breaks rejoining. J Biol Chem 279:55117–55126.

Augustin A, Spenlehauer C, Dumond H, Ménissier-de Murcia J, Piel M, Schmit AC, Apiou F, Vonesh JL, Kock M, Bornens M, de Murcia G. 2003. PARP-3 localizes

preferentially to the daughter centriole and interferes with the G1/S cell cycle progression. J Cell Sci 116:1551–1562.

Boulikas T. 1990. Poly(ADP-ribosylated) histones in chromatin replication. J Biol Chem 265:14638–14647.

Chang YL, Peng YH, Pan IC, Sun DS, King B, Huang DH. 2001. Essential role of *Drosophila* Hdac1 in homeotic gene silencing. Proc Natl Acad Sci 98:9730–9735.

Chang P, Jacobson MK, Mitchison TJ. 2004. Poly(ADP-ribose) is required for spindle assembly and structure. Nature 432:645–649.

Chi NW, Lodish HF. 2000. Tankyrase is a Golgi-associated mitogen-activated protein kinase substrate that interacts with IRAP in GLUT4 vesicles. J Biol Chem 275: 38437–38444.

Cook BD, Dynek JN, Chang W, Shostak G, Smith S. 2002. Role for the related poly(ADP-ribose) polymerases tankyrases 1 and 2 at human telomeres. Mol Cell Biol 22: 332–342.

D'Amours D, Desnoyers S, D'Silva I, Poirier GG. 1999. Poly(ADP-ribosyl)ation reactions in the regulation of nuclear functions. Biochemical J 342:249–268.

Dantzer F, Giraud-Panis MJ, Jaco I, Amé JC, Schultz I, Blasco M, Koering CE, Gilson E, Ménissier-de Murcia J, de Murcia G, Schreiber V. 2004. Functional interaction between poly(ADP-ribose) polymerase 2 (PARP-2) and TRF2: PARP activity negatively regulates TRF2. Mol Cell Biol 24:1595–1607.

Dynek JN, Smith S. 2004. Resolution of sister telomere association is required for progression through mitosis. Science 304:97–100.

Eng J, McCormack A, Yates JR III. 1994. An approach to correlate tandem mass spectral data of peptides with amino acid sequences in a protein database. J Am Soc Mass Spectrom 5:976–989.

Galande S, Kohwi-Shigematsu T. 1999. Poly(ADP-ribose) polymerase and Ku autoantigen form a complex and synergistically bind to matrix attachment sequences. J Biol Chem 274:20521–20528.

Hassa PO, Buerki C, Lombardi C, Imhof R, Hottiger MO. 2003. Transcriptional coactivation of nuclear factor-kappaB-dependent gene expression by p300 is regulated by poly(ADP)-ribose polymerase-1. J Biol Chem 278: 45145–45153.

Huber A, Bai P, Ménissier-de Murcia J, de Murcia G. 2004. PARP-1, PARP-2 and ATM in the DNA damage response: Functional synergy in mouse development. DNA Repair 3:1103–1108.

Johansson M. 1999. A human poly(ADP-ribose) polymerase gene family (ADPRTL): cDNA cloning of two novel poly(ADP-ribose) polymerase homologues. Genomics 57:442–445.

Ju BG, Solum D, Song EJ, Lee KJ, Rose DW, Glass CK, Rosenfeld MG. 2004. Activating the PARP-1 sensor component of the groucho/TLE1 corepressor complex mediates a CaMKinase IIdelta-dependent neurogenic gene activation pathway. Cell 119:815–829.

Keller A, Nesvizhskii AI, Kolker E, Aebersold R. 2002. Empirical statistical model to estimate the accuracy of peptide identifications made by MS/MS and database search. Anal Chem 74:5383–5392.

Kersey PJ, Duarte J, Williams A, Karavidopoulou Y, Birney E, Apweiler R. 2004. The International Protein Index: An integrated database for proteomics experiments. Proteomics 4:1985–1988.

Kickhoefer VA, Siva AC, Kedersha NL, Inman EM, Ruland C, Streuli M, Rome LH. 1999. The 193-kD vault protein, VPARP, is a novel poly(ADP-ribose) polymerase. J Cell Biol 146:917–928.

Kim MY, Mauro S, Gévry N, Lis JT, Kraus WL. 2004. NAD^+-dependent modulation of chromatin structure and transcription by nucleosome binding properties of PARP-1. Cell 119:803–814.

Kozak M. 1989. The scanning model for translation: An update. J Cell Biol 108:229–241.

Kozak M. 1995. Adherence to the first-AUG rule when a second AUG codon follows closely upon the first. Proc Natl Acad Sci USA 92:2662–2666.

Leppard JB, Dong Z, Mackey ZB, Tomkinson AE. 2003. Physical and functional interaction between DNA ligase IIIalpha and poly(ADP-ribose) polymerase 1 in DNA single-strand break repair. Mol Cell Biol 23:5919–5927.

Levine SS, King IFG, Kingston RE. 2004. Division of labor in Polycomb group repression. Trends Biochem Sci 29: 478–485.

Li B, Navarro S, Kasahara N, Comai L. 2004. Identification and biochemical characterization of a Werners's syndrome protein complex with Ku70/80 and poly(ADP-ribose) polymerase-1. J Biol Chem 279:13659–13667.

Maeda Y, Hunter TC, Loudy DE, Davé V, Schreiber V, Whitsett JA. 2006. PARP-2 interacts with TTF-1 and regulates expression of surfactant protein-B. J Biol Chem 281:9600–9606.

Matsui T, Segall J, Weil PA, Roeder RG. 1980. Multiple factors required for accurate initiation of transcription by purified RNA polymerase II. J Biol Chem 255:11992–11996.

Meder VS, Boeglin M, de Murcia G, Schreiber V. 2005. PARP-1 and PARP-2 interact with nucleophosmin/B23 and accumulate in transcriptionally active nucleoli. J Cell Biol 118:211–222.

Ménissier-de Murcia J, Ricoul M, Tartier L, Niedergang C, Huber A, Dantzer F, Schreiber V, Amé JC, Dierich A, LeMeur M, Sabatier L, Chambon P, de Murcia G. 2003. Functional interaction between PARP-1 and PARP-2 in chromosome stability and embryonic development in mouse. EMBO J 22:2255–2263.

Nesvizhskii AI, Keller A, Kolker E, Aebersold R. 2003. A statistical model for identifying proteins by tandem mass spectrometry. Anal Chem 75:4646–4658.

Oei SL, Shi Y. 2001. Transcription factor Yin Yang 1 stimulates poly(ADP-ribosyl)ation and DNA repair. Biochem Biophys Res Comm 284:450–454.

Oei SL, Griesenbeck J, Schweiger M, Ziegler M. 1998. Regulation of RNA polymerase II-dependent transcription by poly(ADP-ribosyl)ation of transcription factors. J Biol Chem 273:31644–31647.

Ogata N, Ueda K, Kawaichi M, Hayaishi O. 1981. Poly(ADP-ribose) synthase, a main acceptor of poly (ADP-ribose) in isolated nuclei. J Biol Chem 256:4135–4137.

Olfert ED, Cross BM, McWilliam AA, editors. 1993. Guide to the care and use of experimental animals. Ottawa: Canadian Council on Animal Care, 195 p.

Otto H, Reche P, Bazan F, Dittmar K, Haag F, Koch-Nolte F. 2005. In silico characterization of the family of

PARP-like poly(ADP-ribosyl)transferases (pARTs). BMC Genomics 6:139.

Ou YY, Mack GJ, Zhang M, Rattner JB. 2002. CEP110 and ninein are located in a specific domain of the centrosome associated with centrosome maturation. J Cell Sci 115:1825–1835.

Rouleau M, Aubin RA, Poirier GG. 2004. Poly(ADP-ribosyl)ated chromatin domains: Access granted. J Cell Sci 117:815–825.

Ruscetti T, Lehnert BE, Halbrook J, Trong HL, Hoekstra MF, Chen DJ, Peterson SR. 1998. Stimulation of the DNA-dependent protein kinase by poly(ADP-ribose) polymerase. J Biol Chem 273:14461–14467.

Saurin AJ, Shiels C, Williamson J, Satijn DPE, Otte AP, Sheer D, Freemont PS. 1998. The human Polycomb group complex associates with pericentromeric heterochromatin to form a novel nuclear domain. J Cell Biol 142:887–898.

Sbodio JI, Lodish HF, Chi NW. 2002. Tankyrase-2 oligomerizes with tankyrase-1 and binds to both TRF1 (telomere-repeat-binding factor 1) and IRAP (insulin-responsive aminopeptidase). Biochem J 361:451–459.

Schreiber V, Amé JC, Dollé P, Schultz I, Rinaldi B, Fraulob V, Ménissier-de Murcia J, de Murcia G. 2002. Poly(ADP-ribose) polymerase-2 (PARP-2) is required for efficient base excision DNA repair in association with PARP-1 and XRCC1. J Biol Chem 277:23028–23036.

Shall S, de Murcia G. 2000. Poly(ADP-ribose) polymerase-1: What have we learned from the deficient mouse model? Mutation Res 460:1–15.

Smith S, de Lange T. 1999. Cell cycle dependent localization of the telomeric PARP, tankyrase, to nuclear pore complexes and centrosomes. J Cell Sci 112:3649–3656.

Sucharov CC, Helmke SM, Langer SJ, Perryman MB, Bristow M, Leinwand L. 2004. The Ku protein complex interacts with YY1, is up-regulated in human heart failure and represses α myosin heavy-chain gene expression. Mol Cell Biol 24:8705–8715.

Tulin A, Spradling A. 2003. Chromatin loosening by poly(ADP-ribose) polymerase (PARP-1) at *Drosophila* puff loci. Science 299:560–562.

Urbanek P, Paces J, Kralova J, Dvorak M, Paces V. 2002. Cloning and expression of PARP-3 (Adprt3) and U3-55k, two genes closely linked on mouse chromosome 9. Folia Biol (Praha) 48:182–191.

Veuger SJ, Curtin NJ, Smith GCM, Durkacz BW. 2004. Effects of novel inhibitors of poly(ADP-ribose) polymerase-1 and the DNA-dependent protein kinase on enzyme activities and DNA repair. Oncogene 23:7322–7329.

Von Haller PD, Yi E, Donohoe S, Vaughn K, Keller A, Nesvizhskii AI, Eng J, Li XJ, Goodlett DR, Aebersold R, Watts JD. 2003. The application of new software tools to quantitative protein profiling via isotope-coded affinity tag (ICAT) and tandem mass spectrometry: II. evaluation of tandem mass spectrometry methodologies for large-scale protein analysis, and the application of statistical tools for data analysis and interpretation. Mol Cell Proteomics 2:428–442.

Woodard RL, Lee KJ, Huang J, Dynan WS. 2001. Distinct roles for Ku protein in transcriptional reinitiation and DNA repair. J Biol Chem 276:15423–15433.

Yu M, Schreek S, Cerni C, Schamberger C, Lesniewicz K, Poreba E, Vervoorts J, Walsemann G, Grotzinger J, Kremmer E, Mehraein Y, Mertsching J, Kraft R, Austen M, Luscher-Firzlaff J, Luscher B. 2005. PARP-10, a novel Myc-interacting protein with poly(ADP-ribose) polymerase activity, inhibits transformation. Oncogene 24: 1982–1993.

Ziegler M, Oei SL. 2001. A cellular survival switch: Poly(ADP-ribosyl)ation stimulates DNA repair and silences transcription. BioEssays 23:543–548.